Available online at www.sciencedirect.com

ScienceDirect

Ceramics International 36 (2010) 121–127

CERAMICS INTERNATIONAL

www.elsevier.com/locate/ceramint

Preparation, sintering and electrical properties of nano-grained multidoped ceria

S. Bošković [a,*], S. Zec [a], G. Branković [b], Z. Branković [b], A. Devečerski [a], B. Matović [a], F. Aldinger [c]

[a] *Institute of Nuclear Sciences Vinca, POB 522, 11001 Belgrade, Serbia*
[b] *Institute for Multidisciplinary Studies, Belgrade, Serbia*
[c] *Max/Planck Institute für Metallforschung, PML, 70569 Stuttgart, Heissenbergstr. 3, Germany*

Received 12 February 2009; received in revised form 25 May 2009; accepted 4 July 2009
Available online 11 August 2009

Abstract

Multiply doped ceria nanopowders were synthesized by applying MGNP (modified glycine/nitrate procedure). The overall concentration of dopants was kept constant ($x = 0.2$) whereby Gd ion as the main dopant was gradually substituted by Sm and by Sm + Y. The compositions of solid solutions were calculated by applying defect model introducing anion vacancy radius. Characterization of powders involved BET, TEM, XRD and chemical analyses. Densification was performed at 1500 °C, in an oxygen atmosphere for 1 h. The results showed that with increasing number of dopants, specific surface area of powders increased, followed by decrease of crystallite and grain sizes. Densification degree was also found to rise with increasing number of dopants. According to impedance measurements it was found that ionic conductivity was the highest 1.14×10^{-3} S cm^{-1} at 450 °C in sample doped with Gd, Sm and Y simultaneously.

Keywords: Nanometric powders; Multiple doping; Densification; Electrical conductivity

1. Introduction

Ceria solid solutions exhibit fluorite type crystal structure and higher electrical conductivity at intermediate temperatures than zirconia for the same dopants concentration which makes them promising candidates for electrochemical devices. Rare earth cations are easily accommodated in the ceria lattice within wide range of concentrations which is followed by increased electrical conductivity.

In general, the conductivity of real systems is dependent on the ceramic processing, as well as on intrinsic properties of the material itself. Density and microstructure features as grain size and grain boundary fraction belong to the first group while the concentration of mobile point defects caused by the type and concentration of dopants belong to the other one.

Microstructure features like grain size and grain boundaries fraction play important role in the conductivity. The conductivity in the nanocrystalline grain boundary regions is greater than for larger grains [1]. That is why high quality powders with particle size in the nanometric range have to be developed and sintering conditions have to be found under which densification will be fast whereas the grain growth process will be inhibited. In such a way, we believe, the quality ceramics could be produced, which will be suitable for SOFC application as an electrolyte, not only because higher electrical conductivity is expected, but also because better mechanical properties may be developed in nanocrystalline ceramics.

The ionic conductivity is realized by oxygen ion movement via oxygen vacancies present in the material as an intrinsic property representing the second group of factors. Doping of ceria with aliovalent cations like rare earth cations (Re) provokes the formation of additional anion vacancies for the sake of electroneutrality. Theoretically the higher the dopants concentration the higher will be the ionic conductivity. In addition, it should be outlined that the conductivity depends not only on the concentration but also on the type, i.e, the size of the dopant cation which represents very important parameter [2]. However, doped ceria on the other hand easily develops

---

* Corresponding author. Tel.: +381 112439454; fax: +381 112430454.
E-mail address: boskovic@vinca.rs (S. Bošković).

0272-8842/$36.00 © 2009 Elsevier Ltd and Techna Group S.r.l. All rights reserved.
doi:10.1016/j.ceramint.2009.07.015

electronic conductivity at high temperatures. It was reported that this problem could be overcome by multiple doping. Literature data showed [3] that Gd, Sm and Y do suppress electronic conduction in single doped ceria and are reported to increase the overall electrical conductivity [4]. Gadolinia doped ceria with $x = 0.2$ is acknowledged to be the single doped material on the basis of ceria with the highest conductivity [4–7]. Also very good results were obtained with Sm doped ceria, as well as with Y doped ceria.

Studying the synthesis, sintering and properties of multi-doped ceria are not very common at the time being, although it was published [3,4] that the electrical conductivity of co-doped ceria increased by up to 30% in comparison with the best single doped material.

Bearing the above said in mind, we studied in this paper, properties of nanosized powders, their densification and properties of ceramics—$Ce_{1-x}Me_xO_{2-\delta}$ with $x = 0.2$, which is known as optimum dopants concentration for many cations in fluorite ceria lattice. Contrary to other methods, modified glycine/nitrate procedure (MGNP) [8,9] applied in this work to synthesize multidoped ceria powders with three dopants simultaneously is very fast and reliable method whereby the needed equipment is extremely simple and inexpensive.

In the studied composition $Ce_{1-x}Gd_xO_{2-\delta}$ Gd ion was gradually replaced by Sm, giving twofold doped solid solution, $Ce_{1-x}(Gd,Sm)_xO_{2-\delta}$, and subsequently by Y, making $Ce_{1-x}(Gd,Sm,Y)_xO_{2-\delta}$, i.e. triple doped ceria solid solutions. Sintering of the mentioned nanopowders was studied at 1500 °C in oxygen atmosphere, as a function of composition as well as of green density. Electrical conductivity of high density samples only was measured by applying impedance spectroscopy.

2. Experimental

Starting chemicals used for the synthesis of powders by MGNP [8,9] were glycine, cerium acetate hydrate, cerium nitrate hexahydrate and Re nitrates hexahydrates (Y, Gd, Sm), produced by Alfa Aesar GmbH, Germany. Reacting solution consisted of Ce-acetate, Ce-nitrate, Re-nitrate and glycine, with small amount of distilled water. All the nitrate solutions both of Ce, and each of the rare earths added to ceria were previously prepared and the cation concentration (in mg/ml) was determined by titration with EDTA. On the basis of these data, the portions of prepared solutions were taken according to previously calculated composition of the final powder [10]. The taken portions of all the nitrates were put into a reactor made of stainless steel. This liquid mixture consisting of all the dopants, independent of their number, was heated on a hot plate. It is obvious that being in the state of water solution, the reacting mixture enables very good homogenization of all the reacting species. The burn-up process of the reacting liquid mixture was terminated at about 450 °C in several minutes. Further details on the modification of the process were published in Refs. [8,9]. As a result of the modifying the reactions proceeded very smoothly. Therefore, almost no loss in the synthesized powders quantity was observed. The powder output was in the range from 96 to 99%, i.e. very close to the theoretical calculations. For practical reasons it is very important to point out that the quantity of chemicals was designed to synthesize 100 g of powder per run (in 30 min), which, presumably, is the largest scale produced by this method so far. The obtained ashes were afterwards calcined at 600 °C for 4 h. The following compositions were prepared:

single-$Ce_{0.8}Gd_{0.2}O_{2-\delta}$,
double-$Ce_{0.8}Gd_{0.12}Sm_{0.08}O_{2-\delta}$ and
triple doped-$Ce_{0.8}Gd_{0.01}Sm_{0.01}Y_{0.18}O_{2-\delta}$.

For comparison pure CeO_2 was produced in the same way. Characterization of the powders involved measurements of specific surface area by BET method, crystal structure analysis by XRD, TEM analysis for particle size and shape observation. Dopants concentration in the final solid solution powders was determined by EDTA titration.

Green pellets were prepared by uniaxial pressing followed by cold isostatic pressing under 225 MPa. Sintering was performed at 1500 °C for 1 h in oxygen atmosphere. The heating rate up to sintering temperature was 5°/min. Density measurement was done by applying Archimedes method. Sintered samples were analyzed by XRD to find out whether possible phase separation took place. Some of the sintered samples were observed under SEM to observe grains size and shape. Electrical conductivity was measured for double and triple doped samples by applying impedance spectroscopy method. The measurement of spectra was carried out in the temperature range 200–600 °C in air atmosphere using HP 4194A equipment under 100 Hz to 1 MHz frequency.

3. Results and discussion

3.1. Powder characterization

All the powders processed by MGNP procedure were voluminous and crystalline with the significant X-Ray lines broadening effect that implies nanometric particle size, which can be seen in Fig. 1. Calculation of the crystallite size and

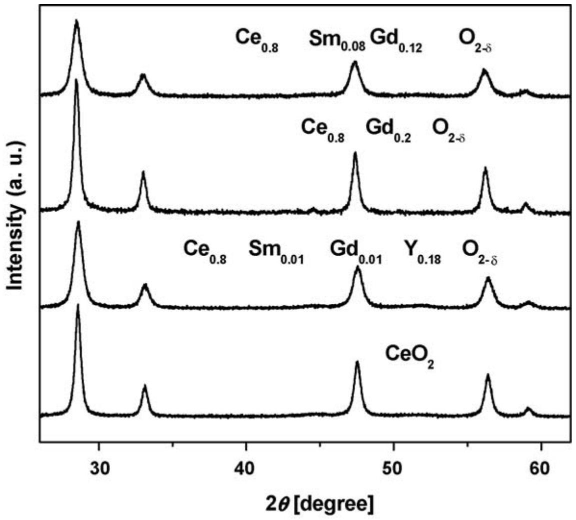

Fig. 1. XRD patterns of nanometric doped ceria powders.

Table 1
Crystallite size, microstrain and specific surface area of powders investigated.

Composition	Lattice parameter (Å)	Crystallite size (Å)	Microstrain ($\times 10^{-3}$)	Specific surface area (m^2/g)
CeO_2 pure	5.412	16.86	11.8	38.26
$Ce_{0.8}Gd_{0.2}O_{2-\delta}$	5.432	19.20	3.4	35.94
$Ce_{0.8}Sm_{0.08}Gd_{0.12}O_{2-\delta}$	5.427	10.15	28.8	51.86
$Ce_{0.8}Sm_{0.01}Gd_{0.01}Y_{0.18}O_{2-\delta}$	5.412	10.10	34.3	49.44

lattice distortion was performed on the basis of the full width at half maximum intensity (FWHM) of the 1 1 1, 2 0 0, 2 2 0 and 3 1 1 peaks of CeO_2 applying Williamson–Hall method and Cauchy expression [11]:

$$\beta \cos\theta = \left(\frac{K\lambda}{D}\right) + 4\varepsilon \sin\theta$$

in which the total peak broadening (β) is the sum of peak broadening due to crystallite size (D) and lattice distortion (ε). Elimination of the instrumental broadening was done using an empirical formula: $\beta = B - b^2/B$, where B represents the measured peak width, while b is the instrumental width obtained from a Si standard. The shown patterns indicate that the crystallite size decreases with increasing number of dopants in multiply doped ceria. Crystallite sizes determined on the basis of XRD data given in Table 1 prove this indication. Obviously, the crystallite size decreases in multidoped compositions $Ce_{0.8}Sm_{0.08}Gd_{0.12}O_{2-\delta}$ and $Ce_{0.8}Sm_{0.01}Gd_{0.01}Y_{0.18}O_{2-\delta}$, when compared to pure ceria.

Specific surface area values of the studied powders are in accordance with our previous data [12,13] and as expected they increase in multidoped powders respective to undoped ceria.

Lattice parameters values of starting powders calculated on the basis of these XRD data are included in Table 1. It can be seen that the lattice parameter increases with doping, but can be kept unchanged related to pure ceria by adjusting the dopants fractions. The optimum composition $Ce_{0.8}Sm_{0.01}Gd_{0.01}Y_{0.18}O_{2-\delta}$ was calculated, as mentioned by applying the ion packaging model [10].

TEM micrographs show (Fig. 2) that the particle size of the synthesized powders is nanometric indeed, and gradually decreases with increasing number of dopants.

To check the precision at which the synthesized compositions were produced, chemical analysis was performed. Existing cations concentrations were determined by EDTA titration. Chosen final compositions were tested and compared to nominal ones.

On the basis of the results given in Table 2, resulting compositions for tested samples were calculated and are:

$Ce_{0.815}Gd_{0.008}Sm_{0.007}Y_{0.17}O_{2-\delta}$ and
$Ce_{0.82}Gd_{0.11}Sm_{0.07}O_{2-\delta}$.

These final compositions show that by applying MGNP procedure for powder synthesis, rather good agreement between nominal and final compositions can be achieved.

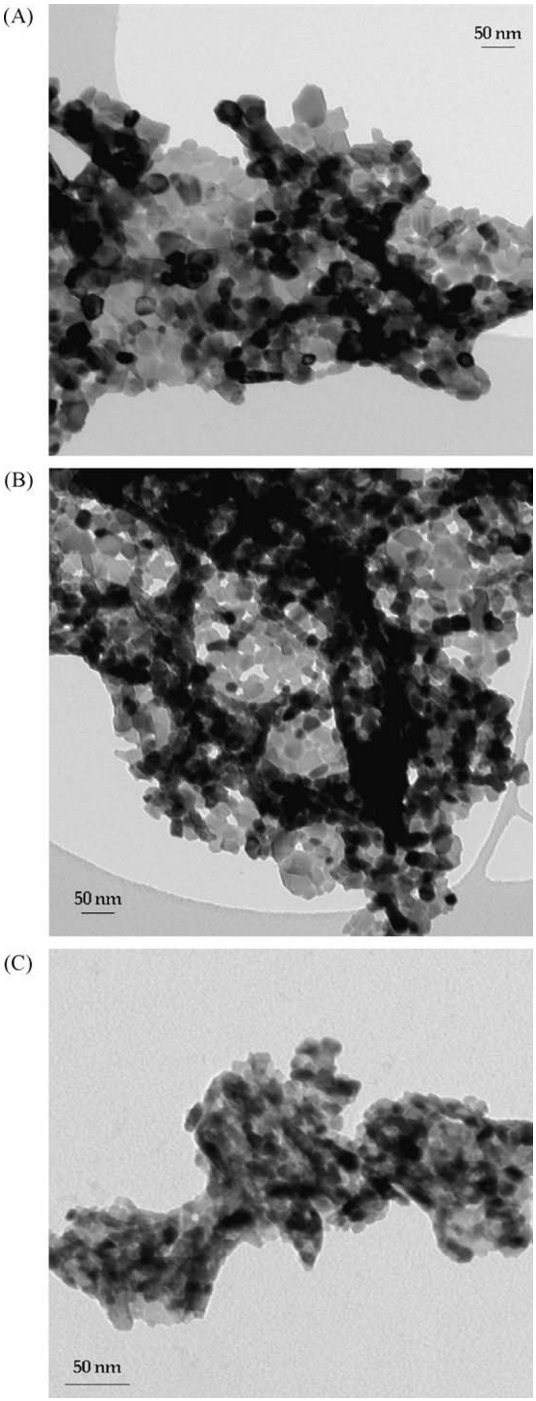

Fig. 2. TEM of (A) CeO_2, (B) $Ce_{0.8}Gd_{0.2}O_{2-\delta}$, and (C) $Ce_{0.8}Sm_{0.01}Gd_{0.01}Y_{0.18}O_{2-\delta}$.

Table 2
Chemical analysis of the produced powders (mass%).

Composition	Ce	Sm	Gd	Y
$Ce_{0.8}Sm_{0.01}Gd_{0.01}Y_{0.18}O_{2-\delta}$	66.0	0.75	0.92	10.9
$Ce_{0.8}Sm_{0.08}Gd_{0.12}O_{2-\delta}$	66.0	7.12	11.9	–

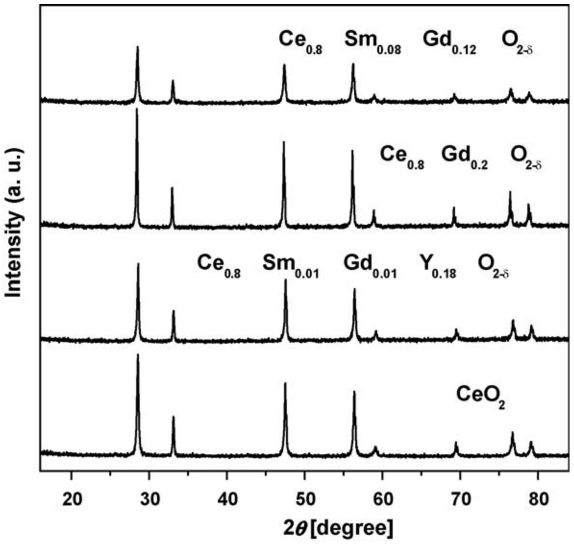

Fig. 3. XRD pattern of sintered samples.

3.2. Densification

The synthesized powders were isostatically cold compacted under 225 MPa, and sintered in a horizontal furnace at 1500 °C, for 1 h, while heating rate was 5°/min. The XRD patterns of sintered samples (Fig. 3) illustrate that crystal structure of the studied compositions being cubic remained unchanged compared to starting powders. In addition single phase composition is proved, too and even lattice parameters were very close to those measured for starting powders (Table 3).

Sintering as described was carried out under the conditions found earlier by studying shrinkage behavior of ceria at different heating rates and different atmospheres [14]. It was proved that under oxygen atmosphere densification of ceria was more intense (Fig. 4) as compared to the results obtained in air. This, however, is not consistent with some literature data [15] according to which density increased due to reduction of ceria which is followed by anion vacancies formation. It is said that accelerated sintering accompanied by oxygen release is due to enhanced bulk diffusion in non-stoichiometric ceria. Contrary to that previous data [14] showed that densities of nanopowder compacts did not decrease in oxygen atmosphere. Density increased in comparison with values obtained in air, although the non-stoichiometry as shown in Fig. 4 increased in air with increasing temperature.

Table 3
Lattice parameters of starting powders and powder compacts sintered at 1500 °C, 1 h.

Composition	Starting powder (Å)	Sintered sample (Å)
CeO_2	5.412	5.413
$Ce_{0.8}Gd_{0.2}O_{2-\delta}$	5.432	5.430
$Ce_{0.8}Gd_{0.12}Sm_{0.08}O_{2-\delta}$	5.427	5.424
$Ce_{0.8}Sm_{0.01}Gd_{0.01}Y_{0.18}O_{2-\delta}$	5.412	5.412

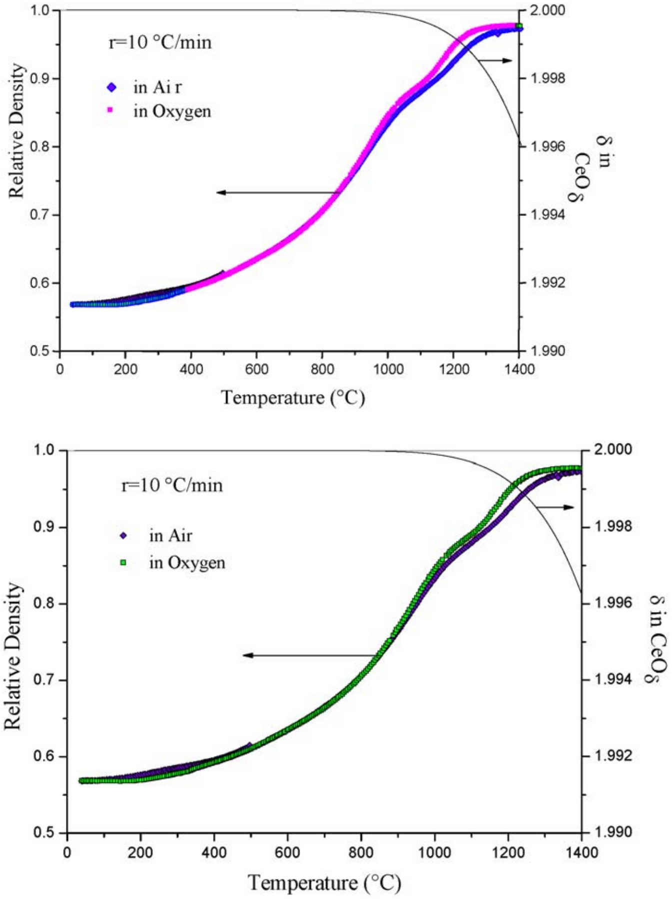

Fig. 4. Density of samples sintered at a constant heating rate in air and oxygen atmosphere and calculated non-stoichiometry of $CeO_{2-\delta}$ in air as a function of sintering temperature [14].

Accordingly, it is believed like in [16] that due to a redox reaction densification was retarded. The reason may be searched in the intensified surface diffusion in non-stoichiometric ceria, which exhibits an inhibiting effect to volume diffusion due to decreasing of neck curvature.

Our further experiments were performed in a dilatometer at different heating rates in oxygen atmosphere up to 1500 °C, which is illustrated for the composition $Ce_{0.8}Sm_{0.01}Gd_{0.01}Y_{0.18}O_{2-\delta}$ in Fig. 5. The results show that sintering started at about

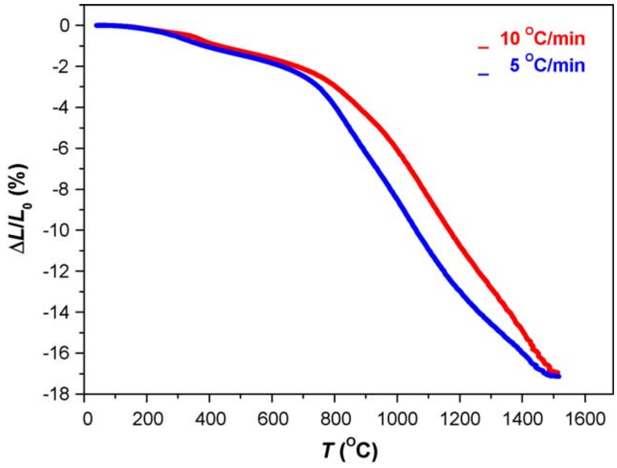

Fig. 5. Shrinkage curves in oxygen for $Ce_{0.8}Sm_{0.01}Gd_{0.01}Y_{0.18}O_{2-\delta}$.

Table 4
Green and sintered densities as well as d_s–d_i parameter, 1500 °C, 1 h.

Composition	d_i TD (%)	d_s TD (%)	d_s–d_i (%)
$Ce_{0.8}Sm_{0.01}Gd_{0.01}Y_{0.18}O_{2-\delta}$	39.89	95.14	55.25
$Ce_{0.8}Sm_{0.08}Gd_{0.12}O_{2-\delta}$	41.49	97.31	55.82
$Ce_{0.8}Gd_{0.2}O_{2-\delta}$	40.82	88.60	47.78
CeO_2	45.64	91.35	45.71

d_s, sintered density; d_i, green density.

300 °C something earlier with samples heated at 5°/min. It is also to see that more intense shrinkage took place at a lower heating rate. Shrinkage degree became equal independent of heating rate at the end of process at 1500 °C. On the basis of these results our sintering experiments were carried out at 5°/min heating rate, in oxygen atmosphere, at 1500 °C for 1 h in an electroresistant furnace. In Table 3 lattice parameters of starting and sintered samples are summarized for different compositions. It can be seen that lattice parameter increases with doping, but can be kept the same as in pure ceria (tripple doped sample) by adjusting the dopants fractions. This composition was calculated, as mentioned by applying ion packaging model [10]. In Table 4 the green and sintered densities for different compositions are given that were obtained under the same conditions. Densification degree d_s–d_i, is included, too. Obviously the samples with very low green densities can be sintered up to high densification levels, as previously stated by Chen and Chen [17]. It was found that the degree of densification increases with increasing number of dopants, which is obvious from densification parameter value which in our case better describes the influence of dopants on the densification, because it eliminates the influence of green density variation. The obtained results are consistent with characteristics of powders shown in previous part. Namely, with increasing number of dopants, the specific surface area increases, while particle and crystallite sizes decrease. These properties are very relevant for sinterability. Except for favorable powder properties it is difficult to judge on the basis of the present data the influence of increased number of dopants on densification, because their total concentration is kept constant throughout the study. The fact is that by introducing three valent cations into the ceria lattice, oxygen vacancies are

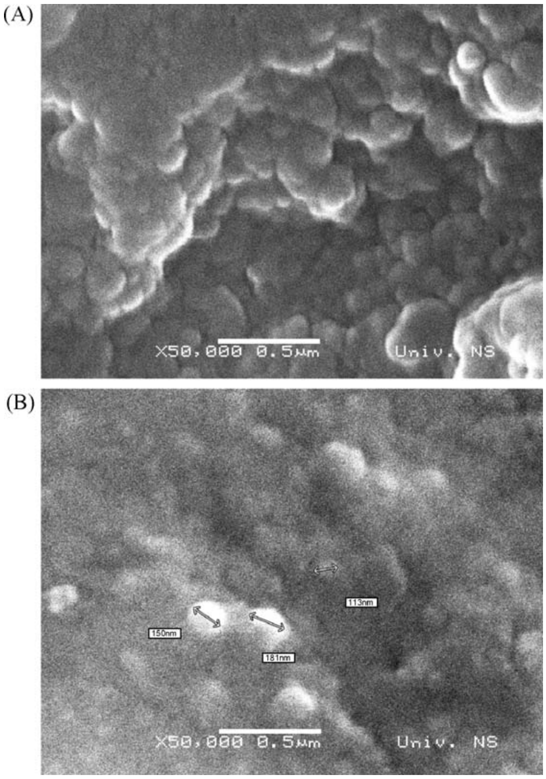

Fig. 6. SEM micrographs of the fractured surface of $CeO_{2-\delta}$ (A) and $Ce_{0.8}Sm_{0.01}Gd_{0.01}Y_{0.18}O_{2-\delta}$ (B), 1500 °C, oxygen atmosphere.

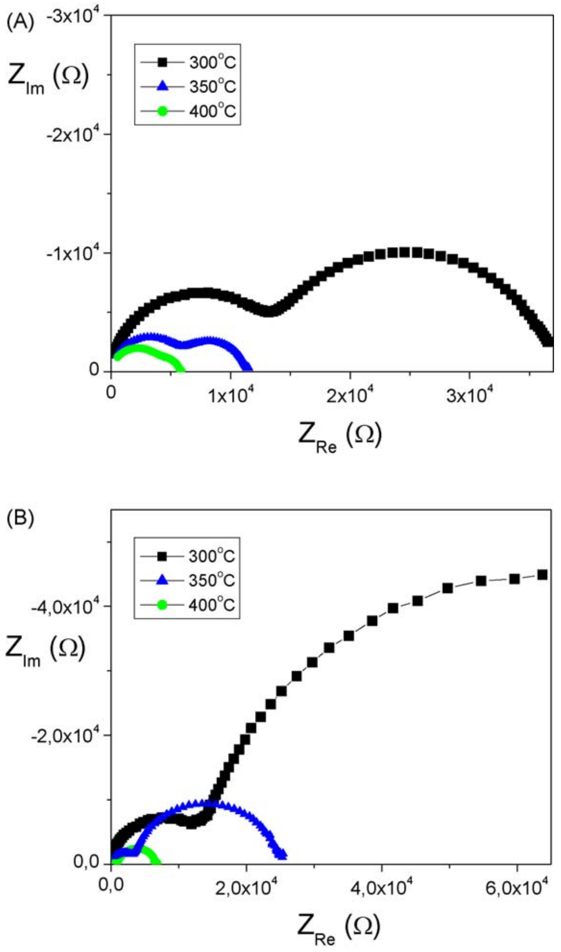

Fig. 7. Impedance spectra for $Ce_{0.8}Sm_{0.08}Gd_{0.12}O_2$ (A) and for $Ce_{0.8}Sm_{0.01}Gd_{0.01}Y_{0.18}O_{2-\delta}$ (B).

Table 5
Densities and volume shrinkage for different pressing pressures.

Composition	d_i TD (%)	d_s TD (%)	$\Delta V/V_0$ (%)
$Ce_{0.8}Nd_{0.01}Sm_{0.015}Gd_{0.025}Dy_{0.04}Y_{0.05}Yb_{0.06}O_{2-\delta}$[a]	35.66	89.43	61.36
$Ce_{0.8}Nd_{0.01}Sm_{0.015}Gd_{0.025}Dy_{0.04}Y_{0.05}Yb_{0.06}O_{2-\delta}$[b]	37.47	81.08	44.86
$Ce_{0.8}Sm_{0.08}Gd_{0.12}O_{2-\delta}$[a]	40.09	99.1	61.42
$Ce_{0.8}Sm_{0.08}Gd_{0.12}O_{2-\delta}$[b]	41.77	97.3	56.26

[a] 130 MPa.
[b] 225 MPa.

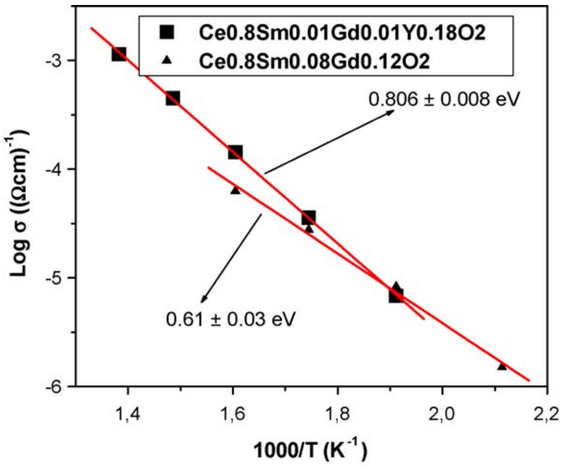

Fig. 8. Arrhenius plot for ionic conductivities of co-doped sintered samples $Ce_{0.8}Sm_{0.08}Gd_{0.12}O_{2-\delta}$ and $Ce_{0.8}Sm_{0.01}Gd_{0.01}Y_{0.18}O_{2-\delta}$.

Table 6
Bulk conductivities σ (S cm^{-1}).

T (°C)	$Ce_{0.8}Sm_{0.08}Gd_{0.12}O_{2-\delta}$	$Ce_{0.8}Sm_{0.01}Gd_{0.01}Y_{0.18}O_{2-\delta}$
200	1.50×10^{-6}	
250	8.29×10^{-6}	6.82×10^{-6}
300	2.76×10^{-5}	3.75×10^{-5}
350	6.29×10^{-5}	1.43×10^{-4}
400	9.75×1^{-5}	4.49×10^{-4}
450	1.56×10^{-4}	1.14×10^{-3}

created according to

$$2CeO_2 \rightarrow 2\,Re_{Ce'}V_O^{\bullet\bullet} + \tfrac{1}{2}O_2$$

Since the total concentration of dopant cations was kept to a great extent constant (Table 3) the oxygen vacancy concentration must be the same in different compositions and equal to half of the dopants concentration. This could indicate that diffusion of slower species may be enhanced in all the studied compositions. Yet, a difference in densification degree was proved. We believe that different sinterability was mostly due to powder characteristics, as mentioned above, which may be the consequence of the presence of different kinds of dopants.

For practical reasons it was tried to sinter green pellets compacted at much lower pressing pressure under the described sintering conditions. Volume shrinkage depending on pressing pressure (130 and 225 MPa) was followed for two different compositions. It was found that lower density samples can be sintered to high level and that both sintered densities and shrinkage were higher for samples obtained under the lower pressure (Table 5), indicating faster process development. The obtained data seem to support the results in Ref. [17]. In the green compact of nanopowders the rearrangement of particles during sintering is more intense in samples with lower green densities. During the rearrangement process the sliding of particles over each other is more intense in low density compacts since there is much more open space. One can imagine the situation that during these processes the particles achieve best possible packing.

Table 7
Activation energies for bulk (E_g) and grain boundary (E_{gb}) conductivities.

Composition	Ea_b (eV)	Ea_{gb} (eV)
$Ce_{0.8}Sm_{0.08}Gd_{0.12}O_{2-\delta}$	0.66	0.79
$Ce_{0.8}Sm_{0.01}Gd_{0.01}Y_{0.18}O_{2-\delta}$	0.81	0.93

SEM micrographs show that sintering under these conditions produces ceramic material with nanometric grain size (Fig. 6), both in pure ceria as well as in triple doped ceria samples.

3.3. Electrical properties

Electrical conductivity was measured by using an impedance analyzer, as described earlier. The spectra were taken in the temperature range 200–450 °C. The Niquist plots for two co-doped samples with high density level are presented in Fig. 7. It was assumed that the density of single doped sample being relatively low could bring some confusion in conductivity results and therefore it was not analyzed. We intend to change sintering conditions and hope to get higher densities for all samples including single doped ones at considerably lower temperatures. The data show that the contribution of grain boundary conductivity decreases with increasing temperature. From the data in Fig. 7, the conductivities were calculated as a function of temperature and are summarized in Table 6.

The straight line in Fig. 8 for triple doped sample exhibits higher slope indicating faster increase in conductivity with further temperature rise. The maximum value was obtained for triple doped sample (Table 6) that we expected also on the basis of literature data [3] and also on the basis of data which stated that conductivity is higher if the mismatch in ionic radii between host and dopant cation is the lowest [10]. In the case of this composition, it could be outlined that the mismatch between ‘‘effective’’ ionic radius [9] and cerium practically negligible resulting in the unchanged lattice parameter as compared to pure ceria (Table 2). On the other hand it had been reported [18] that Y ion has the ability to form defect complexes. Bearing in mind the conductivity data we obtained, for sample containing Y ion one could speculate that although the three different cations are present in the lattice, whereby one of them Y, is highly dominant dopant, the formation of complexes may not be the case with this combination of ions since the conductivity is quite high (see Table 6). This however, will be proved. The obtained values for activation energy presented in Table 7 correspond to the ionic conductivity and are consistent with published data.

It is interesting to note that the arguments can be found to state that sample processing parameters play more important role than it is generally recognized [19]. In this connection we show the microstructures of sintered samples (in Fig. 6), with about 100 nm grain size, that also positively affects the conductivity as found by [1].

4. Conclusion

Synthesis of multidoped ceria powders was performed by MGNP method. Very fine nanometric powders were obtained, with particles size 15–20 nm and high specific surface area. The obtained powders were single phase and remained single phase after sintering at 1500 °C, in oxygen atmosphere. Low green density pellets from 35 to 41.77/%/TD of nanometric powders achieved high densification levels during sintering. The densification degree increased with increasing number of dopants. It is believed that this was due predominantly because of increased sinterability of powders themselves. The obtained results on conductivity show as well, that with increasing number of dopants the ionic conductivity at higher measuring temperatures increases. This is due to positive effect not only of dopants but also of microstructure parameters. A maximum value of $1.14 \times 10^{-3}\ \mathrm{S\,cm^{-1}}$ was obtained for triple doped sample.

Acknowledgements

The authors respect the support of the project no. 142003 by the Ministry of Science and Technology of Serbia and the Humboldt Foundation. The authors are also grateful to PML staff for the experimental help.

References

[1] M. Oljaca, R. Maric, S. Shanmunghan, A. Hunt, Nanomaterials for solid oxide fuel cells, Am. Ceram. Soc. Bull. 82 (1) (2003) 38–40.

[2] T. Suzuki, I. Kosacki, H.U. Anderson, Defect and mixed conductivity in nanocrystalline doped cerium oxide, J. Am. Ceram. Soc. 85 (6) (2002) 1492–1498.

[3] J. Kim, D. Lee, The effect of multiple doping on electrical conductivity of gadolinia doped ceria electrolyte, Korean J. Chem. Eng. 19 (3) (2002) 421–424.

[4] J. van Herle, D. Senevirante, A.J. McEvoy, Lanthanide co-doping of solid electrolytes: AC conductivity behaviour, J. Eur. Ceram. Soc. 19 (1999) 837–841.

[5] K. Muthukkumaran, P. Kuppusami, E. Mohandas, V.S. Raghunathan, S. Selladurai, Ionic conductivity measurements in gadolinia doped ceria, in: International Symposium on Materials Science and Engineering, Dec. 20–22, Chennai, India, 2004.

[6] E. Gourba, P. Briois, A. Ringuede, M. Cassier, Electrical properties of gadolinia doped-ceria thin films deposited by sputtering in view of SOFC application, J. Solid State Electrochem., doi:10.1007/s10008-004-0503-3.

[7] T.S. Zhang, J. Ma, Y.J. Leng, S.H. Chan, P. Hing, J.A. Kilner, Effect of transition metals oxides on densification and electrical properties of Si-containing $Ce_{0.8}Gd_{0.2}O$ ceramics, Solid State Ionics, doi:10.1016/j.ssi.2004.02.015.

[8] S.B. Bošković, B.Z. Matovic, M.D. Vlajić, V.D. Kristić, Modified glycine nitrate procedure (MGNP) for the synthesis of SOFC nanopowders, Ceram. Int. 33 (1) (2007) 89–93.

[9] S.B. Bošković, D.R. Djurović, S.P. Zec, B.Z. Matović, M. Zinkevich, F. Aldinger, Doped and co-doped CeO_2: preparation and properties, 2007, Ceram. Int. 34 (2008) 2001–2006.

[10] Seong Jae Hong, Anil V. Virkar, Lattice ceria electrolytes, J. Am. Ceram Soc. 78 (1995) 433–439.

[11] B. Lönnberg, Characterization of milled Si_3N_4 powder using X-ray peak broadening and surface area analysis, J. Mater. Sci. 29 (12) (1994) 3224–3230.

[12] S. Boskovic, S. Zec, M. Ninic, J. Dukic, B. Matovic, D. Djurovic, F. Aldinger, Nanosized ceria solid solutions obtained by different chemical routes, J. Optoelectron. Adv. Mater. 10 (3) (2008) 515–519.

[13] S. Bošković, D. Đurović, Z. Dohčević-Mitrović, Z. Popović, M. Zinkevich, F. Aldinger, Self propagating room temperature synthesis of nanopowders for SOFC, J. Power Sources 145 (2) (2005) 237–242.

[14] D. Djurović, M. Zinkevich, S. Bošković, V. Srot, F. Aldinger, Densification behaviour of nano-size CeO_2, Mater. Sci. Forum 518 (2007) 191.

[15] Masakuni Ozawa, Effect of oxygen release on the sintering of fine CeO_2 powder at low temperatures, Scripta Mater. 50 (2004) 61–64.

[16] V. Zhou, M.N. Rahman, Effect of redox reaction on the sintering behaviour of cerium oxide, Acta Mater. 45 (9) (1997) 3635.

[17] P.-L. Chen, I.-W. Chen, Sintering of fine oxide powders: I. Microstructural evolution, J. Am. Ceram. Soc. 79 (12) (1986) 3129–3314.

[18] H. Deguchi, H. Yoshida, T. Inagaki, M. Hirouchi, Solid State Ionics 176 (2005) 1817–1825.

[19] G. Bryan Bazals, R.S. Glass, AC impedance studies of rare earth oxide doped ceria, Solid State Ionics 76 (1955) 155–162.